Experimental and Numerical Studies of Flush Electrostatic Probes in Hypersonic Ionized Flows: I. Experiment

D. W. BOYER*
Cornell Aeronautical Laboratory Inc., Buffalo, N. Y.
AND
K. J. TOURYAN†
Sandia Laboratories, Albuquerque, N. Mex.

Experimental studies were performed to determine the ion current collection characteristics of flush-mounted electrostatic probes on a sharp flat plate in ionized hypersonic flows. The effects of probe size, geometry, position, bias, and local flow properties were explored. The probe current densities measured in nitrogen, argon, and carbon monoxide plasmas were correlated in terms of the flow Reynolds number, electron convective flux, probe size, applied potential and electron-to-ion temperature ratio. The correlation predicts well similar data available in the literature. Comparison with a numerical solution of Poisson's equation yields results which validate the correlation.

Nomenclature

A/A_* = nozzle area ratio
C^* = Chapman-Rubesin constant in the linear viscosity-temperature relation
D = diffusion coefficient
e = electron charge
I = probe current
J = current density
m = exponent in flush-probe current-voltage relationship
M = Mach number
n = number density
p = pressure
R = probe radius
Re = Reynolds number
Sc = Schmidt number
T = temperature
u = flow velocity
V = probe voltage relative to ground
x = distance from plate leading edge
X_N = axial distance from nozzle throat
y = distance normal to surface of flat plate
β = ratio of ion to electron diffusion coefficient
δ = boundary-layer thickness
ε = T_i/T_e
κ = correlation parameter, $(R/\lambda_D)^2\ 1/Re_{x_o}Sc_i$
λ = mean free path
λ_s = sheath thickness
λ_D = Debye length (in general based on boundary-layer edge conditions)
μ = viscosity
ρ = density
$\varphi_p(=-\psi)$ = dimensionless potential difference between probe and undisturbed plasma (relative to T_e)
$\bar{\chi}$ = hypersonic interaction parameter

Subscripts

o = boundary-layer edge value
e = electron
F = value at floating potential
i = ion
n = neutral
p = probe surface
T = translational value
∞ = undisturbed plasma

Presented as Paper 72-104 at the AIAA 10th Aerospace Sciences Meeting, San Diego, Calif., January 17–19, 1972; submitted February 22, 1972; revision received June 28, 1972. This work was supported by the U. S. Atomic Energy Commission.

Index categories: Plasma Dynamics and MHD; Supersonic and Hypersonic Flow.

* Principal Aerodynamicist.

† Manager, Aerodynamics Research Department. Associate Fellow AIAA.

Introduction

AMONG the various types of electrostatic probes used, the flush-mounted or surface electrostatic probe is particularly well suited for measuring the electron number density (or the temperature) in re-entry vehicle plasmas. As the name implies, the flush probe consists of a conductor surrounded by an insulator whose exposed surface is flush with that of the body. When the dimensions of the probe R are small compared to a mean free path λ, it acts as a classical Langmuir probe.[1] For re-entry boundary-layer measurements, however, it is not practical to have $R \ll \lambda$. Furthermore, under most re-entry conditions, the sheath is collision dominated.

Lam,[2] Chung,[3] Denison,[4] and Burke[5] have studied the interation between a solid body and a weakly ionized flowing plasma under the aforementioned conditions. These studies have emphasized the collisional thin sheath case wherein $\lambda_s \ll R < \delta$. Experimental verification has been carried out in shock tubes by Hoppmann,[6] Burke,[7] Scharfman and Bredfeldt.[8] The opposite limit of very thick sheaths has been studied by Sonin[9] and recently by deBoer,[10] Dukowicz,[11] and Hammitt[12] who solved the thick sheath case in the small diffusion limit, assuming the flowfield near the probe surface to be uniform.

The general case of finite sheath thickness $R \leq \lambda_s \leq \delta$ is less well understood. The reason is that one has to solve the complete two- or three-dimensional Poisson equation together with the two-dimensional species continuity equations. Recent shock tube experiments with flush-mounted, constant voltage probes on flat plates by Scharfman and Bredfeldt,[8] Lederman and Avidor[13] have shed some light on the behavior of these probes under finite sheath thickness conditions, but detailed studies of the current-voltage (CV) characteristics, under the condition $R \leq \lambda_s \leq \delta$ is lacking.

The present study is concerned specifically with providing such data. To this end, detailed numerical and experimental studies were performed to determine the current collection characteristics of flush-mounted electrostatic probes installed in the dielectric surface of a sharp leading-edge flat plate in ionized hypersonic boundary layers. The experiments have examined the effect of probe size; geometry; position; bias, and variations in the local boundary-layer properties. The present study is analogous to the experimental and theoretical investigations of conical probes conducted recently by Dukowicz[14] Scharfman and Hammitt.[15]

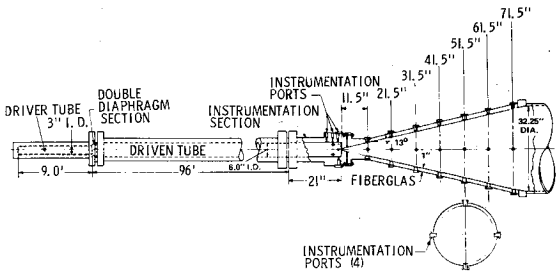

Fig. 1 Schematic of experimental apparatus.

This paper deals with the experimental results. In it we discuss the experimental apparatus, the instrumentation and the various measurements performed. The data are analyzed in the light of existing theories, and recent numerical studies reported in Ref. 33. Results are compared with similar data available in the literature.[7,8,13]

Experimental Apparatus, Method and Scope of Measurements

The investigation to be discussed comprised three series of experiments. In the first series, thin-wire electrostatic probes were used to measure the electron temperature and electron number density profiles in the hypersonic ionized boundary-layer flow over a flat plate. The second series of experiments comprised the measurement of the current-collection characteristics of flush-mounted electrostatic probes, installed on the dielectric surface of the flat plate. The complementary flush probe characteristics and ionized boundary-layer profile measurements were performed in nitrogen and argon and were obtained under similar local plasma conditions over the flat plate. In addition, a few experiments were performed in carbon monoxide in order to record the flush-probe current-voltage characteristics under conditions of higher freestream electron number density than were obtained in argon. The first and second series experiments were performed in a hypersonic nozzle freestream flow under conditions $T_e/T_i > 1$.

The third experimental series was performed in the equilibrium flow behind the incident shock wave in the driven tube of the shock tunnel. These experiments comprised the measurement of the continuum current-voltage characteristics of flush probes installed in a second flat-plate model used in previous studies of the current collection to constant-voltage flush probes in equilibrium air.[7] The present shock tube investigations were performed in nitrogen under conditions $T_e/T_i = 1$.

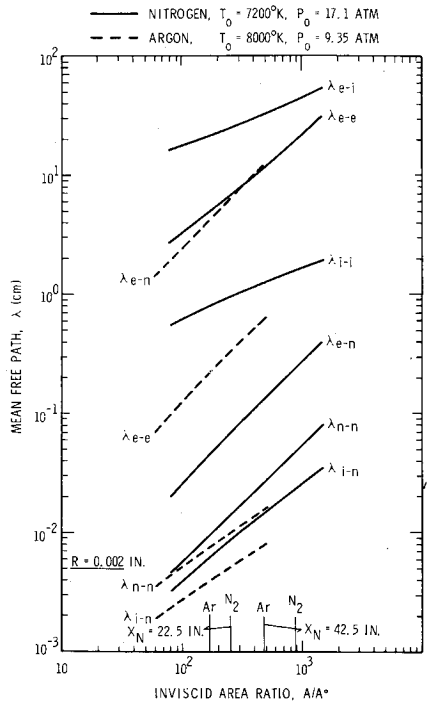

Fig. 2 Calculated mean free path in expanding nitrogen and argon plasmas.

Details of Experimental Apparatus

A schematic diagram of the hypersonic shock tunnel is shown in Fig. 1. The initial pressure conditions in the shock tube provided an equilibrium reservoir state of 7200°K and 17.1 atm pressure in nitrogen, and 8000°K and 9.35 atm pressure in argon. These particular operating conditions were chosen to duplicate those which have been employed in previous investigations of the electron temperature and number density distributions in expanding nitrogen and argon plasmas,[16,17] in which the flow behavior, nozzle starting process and uniform-flow duration have been studied in detail. In order to ensure the attainment of ionization equilibrium in the reservoir gas, a small amount of nitrogen (0.0012 mole) was added to the argon test gas for these experiments.

The calculation of the nonequilibrium nozzle-flow expansions from the nitrogen and argon reservoir states was performed using the computer program described in Ref. 18. The computation assumed thermodynamic equilibration of the vibrational and electronic degrees of freedom with the translational temperature but allows all chemical reactions to proceed at finite rates. These calculations showed the predominant ion in the nitrogen plasma to be N^+ (N_2^+ being unimportant at the nozzle test stations of interest in these experiments), and Ar^+ in argon. The turbulent boundary-layer growth in the nozzle was calculated using the semiempirical method of Burke and Wallace,[19] and the gasdynamic parameter distributions corresponding to the effective inviscid-core area ratio were obtained from the nitrogen and argon nozzle flow calculations. The calculated particle-particle mean free paths in the nitrogen and argon expansions are shown in Fig. 2 as a function of the inviscid area ratio. These values were obtained from the nozzle flow solutions using the relations noted by Sonin.[20]

The experiments in a carbon-monoxide plasma were performed at two reflected-shock reservoir conditions. The first condition, 7300°K and 17.3 atm, was close to that employed in the experiments of Ref. 21, in which the calculated gasdynamic parameter distributions in the nozzle expansion were essentially the same as those in the nitrogen experiments. The second carbon monoxide reservoir condition was 7800°K and 24.2 atm, which afforded the highest freestream number density test condition of the experiments. The dominant ion was C^+ in the carbon monoxide plasma expansions.[21]

Models

The stainless-steel flat-plate model used in the nozzle-flow experiments is shown schematically in Fig. 3. The plate had a span of 7 in. and a length of 13 in. A $\frac{1}{4}$-in.-deep, full-span cutout was machined into the plate surface 3-in. aft of the sharp leading edge to accommodate interchangeable 9-in.-long dielectric inserts. The flush probes were installed in the inserts in groups of up to 5 across the span, at each of two plate stations located 4.5 in. and 9.5 in., respectively, from the leading edge. When installed in the model, the inserts were flush with the plate surface and on the nozzle centerline. In order to encompass a sufficiently large range in collector diameters, the flush probes were distributed over 4 inserts and ranged in diameter from 0.005 in. to 1.25 in. In addition, a fifth insert was employed to investigate the effect of probe geometry on flush-probe current collection and contained three probes, a $\frac{1}{2}$-in.-diam circle, a $\frac{1}{2}$-in. square and a $2 \times \frac{1}{2}$-in. rectangle. In order to minimize the possible complicating effects of run-to-run variations in the test freestream number density on the flush probe measurements, the probe arrangement on one insert was modified during the course of the experiments so as to provide nearly a four-order of magnitude range in flush probe area on the one insert.

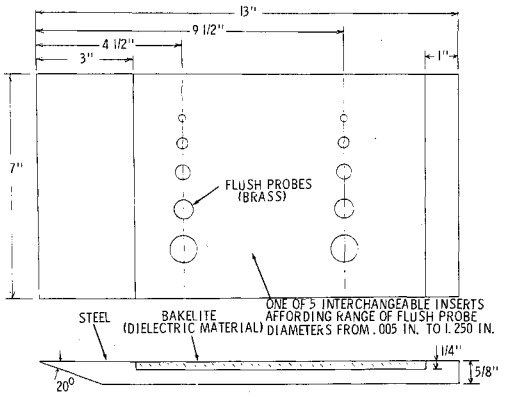

Fig. 3 Schematic of flat plate model and inserts.

The flush probe and boundary-layer electron temperature and number density profile measurements in nitrogen and argon were performed at two stations in the nozzle, in which the plate leading edge was positioned at 22.5 in. and 42.5 in., respectively, from the nozzle throat (Fig. 1). The flush probe experiments in carbon monoxide were performed with the plate leading edge at the $X_N = 22.5$ in. station only. The details of the electrostatic and flush probe measurements, operating technique and data reduction procedures are discussed fully in Ref. 22.

Tunnel Flow Conditions

The integrated freestream electron number density was measured throughout the nozzle experiments by means of two microwave interferometers operated at 17 GHz and 35 GHz, respectively. The 17 GHz interferometer was always located 1 in. upstream of the plate leading edge and the 35 GHz interferometer at the next upstream station in the nozzle (Fig. 1). Typical interferometer records obtained in the nitrogen and argon plasmas are shown in Fig. 4. The test time in the nitrogen (and carbon monoxide) plasmas was about 140 μsec and at least 600 μsec in argon. The interferometrically measured electron number density distributions in the expanding nitrogen and argon plasmas are shown in Fig. 5.

The calculated freestream conditions at the plate leading edge in the nitrogen, argon, and carbon monoxide plasma expansion are presented in Table 1. Some consideration was also given to the calculation of the parameter distributions in flow over the plate. Over the length of the inserts, for example, values of the hypersonic interaction parameter $\bar{\chi} = M_\infty^3 (C^*/Re_{\infty,x})^{1/2}$, ranged from 2.5 to 13 in nitrogen and 7.5 to 45 in argon. Only pressure interaction effects were considered.

The induced pressure field over the plate was calculated using an iterated tangent-wedge expression suitable for the present transitional-range of $\bar{\chi}$ values. In addition, since the expanding flow in the conical nozzle is a source-type flow, a correction was necessary to account for the axial gradients in the freestream flow over the plate (see Burke and Bird[23]).

In view of the simplified nature of the estimates for the plate-flow distributions, it was considered necessary to obtain a corroborative measurement of the pressure distribution over the plate. A total of 8 pressure transducers were, therefore, installed on one of the inserts and the plate centerline pressure distribution as well as the spanwise pressure at locations $\frac{1}{2}$-in. aft of the flush probe stations were measured during the initial experiments. The pressure measurements confirmed the two-dimensionality of the flow over the plate as far back as 10 in. from the leading edge, but also showed a greater axial pressure gradient along the plate surface than that indicated by the source-flow calculations. Based on the measured pressure distribution on the plate, therefore, corrections were made to the previous source-flow estimates for the other gas-dynamic parameter distributions over the plate. The resultant values for the flow parameters at the two-plate stations of interest in these experiments are included in Table 1. These values were then employed as the input edge conditions in the calculation of the nonequilibrium boundary-layer flow in nitrogen and argon, using the computer program described by Blottner[24] adapted to flat plate flows.

Details of the Measurements

The electron temperature and number density profile measurements in the boundary-layer flows on the flat plate were obtained with thin-wire electrostatic probes aligned in the flow direction, parallel to the plate surface. The probe diameters D were 0.004 in. and the probe length l was 0.4 in., affording an l/D ratio of 100.

Table 1 Flow conditions over flat plate

Flat-plate leading-edge Station	Parameter	Nitrogen			Argon			Carbon monoxide			
		Freestream		$X=9.5$ in.	Freestream	$X=4.5$ in.	$X=9.5$ in.	Freestream (A)[a]	Freestream (B)[b]	$X=4.5$ in. (A)[c]	$X=4.5$ in. (B)[c]
$X_N = 22.5$ in.	U, m/sec	4550	4565	4605	2870	2870	2870	4525	4670	4550	4700
	p, atm	1.86×10^{-3}	1.53	0.79	2.8×10^{-4}	8.68	5.6	1.73×10^{-3}	2.42	1.42	2.0
	ρ, g/cm^3	6.2×10^{-7}	5.45	3.5	1.09×10^{-6}	2.07	1.64	6.1×10^{-7}	10	5.35	8.8
	T_T, °K	935	880	690	124	206	166	830	885	780	835
	T_e, °K	2700	2500	2300	1100	1100	1100	2200[a]	~2200	2100[a]	~2200
	μ, g cm/sec	3.8×10^{-4}	3.7	3.2	1.03×10^{-4}	1.67	1.37	3.6×10^{-4}	3.75	3.45	3.61
	M_∞	7.0			13.85			7.2		7.5	
	Re, cm^{-1}	740	670	510	3040	3560	3425	765	1245	705	1145
	n_e, cm^{-3}	$2.2\text{-}2.7\times10^{10}$			$1.4\text{-}2.1\times10^{11}$			3.5×10^{11}[d]	6.2×10^{11}[d]		
$X_N=42.5$ in.	U, m/sec	4645	4645		2880	2880					
	p, atm	3.17×10^{-4}	7.3		5×10^{-5}	4.85×10^{-4}					
	ρ, g/cm^3	1.72×10^{-7}	3.0		3.9×10^{-7}	11.3					
	T_T, °K	565	740		62	208					
	T_e, °K	2200	2200		1000	1000					
	μ, g cm/sec	2.79×10^{-4}	3.3		0.51×10^{-4}	1.68					
	M_∞	9.1			19.65						
	Re, cm^{-1}	285	420		2200	1940					
	n_e, cm^{-3}	$4\text{-}6\times10^9$			$4.5\text{-}5.5\times10^{10}$						

[a] Obtained from nozzle calculations and T_e data of Ref. 21.
[b] Parameters estimated from nozzle calculations for (A).
[c] Parameters estimated from N_2 flat plate calculations.
[d] Measured in present experiments.

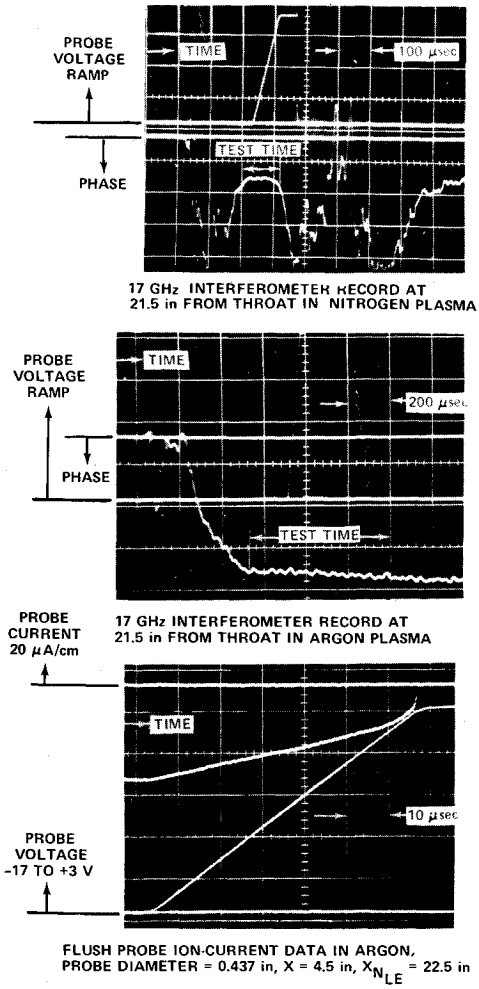

Fig. 4 Typical interferometer and flush probe data.

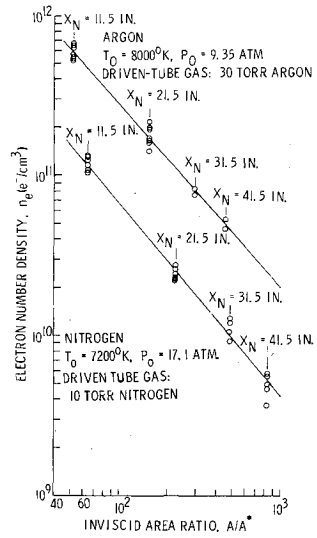

Fig. 5 Measured electron number densities in expanding N_2 and Ar Plasmas.

Previous studies [25] have demonstrated no dependence on the derived electron temperature or number density on the fineness ratio, l/D at l/D values down to 50.

The electron number density was determined from the ion-current portion of the probe characteristic using the theory of Laframboise[26] and the constraints of the probe diameter were twofold. It was necessary that the probe diameter be small enough to ensure that ion-neutral collisions did not significantly influence ion-current collection. On the other hand, in the region of large Debye length close to the plate surface, ratios of probe radius to Debye length, R/λ_D, may approach unity or lower for probe diameters too small. Under these conditions the ion sheath becomes sufficiently thick that ion-current collection may be appreciably enhanced by convection and data interpretation using free-molecular theory will overpredict the number density. This current enhancement corresponds to the end-effect described by Hester and Sonin.[27] The present 0.004 in. probe diameter was selected on the basis of the above considerations.

Reference to Fig. 2 shows that the ion-neutral mean free paths in nitrogen and argon are comparable to the ion-probe radius at the $X_N = 22.5$ in. station indicating that the probe measurements at the first station on the plate were performed in a near-transitional flow regime. The importance of the ion-neutral collisional effects in the derived number density profiles was determined and, when necessary, corrections to the profile measurements were performed using the transitional regime analysis of Talbot and Chou.[28]

The thin-wire probe boundary-layer profile measurements were performed independently of the flush probe measurements in order to ensure that the thin-wire probe data were not influenced by charged-particle migration to local current-collecting flush probes. Except for distances very close to the plate surface, the profile measurements at the $x = 4.5$ in. and 9.5 in. stations were obtained using a rake containing three probes, spaced 1 in. apart. In the larger Debye length region near the wall ($y \lesssim 0.05$ in.), however, only a single probe was used to avoid possible probe interference effects. The voltage applied to the thin wire probes was swept from -5 to $+2$ v, relative to ground, in the nitrogen plasmas, and from -4 to $+4$ v in argon, in a period of about 75 μsec. The probe-voltage sweeps were delayed so as to coincide with the arrival of the uniform test plasma at the particular station on the plate (Fig. 4).

In order to minimize the effect of run-to-run variations in the freestream number density on probe data interpretation, the boundary-layer profile measurements at the $x = 4.5$ in. and 9.5 in. stations on the plate were performed simultaneously during each experiment. Furthermore, since the probes were always aligned parallel to the plate surface, some misalignment of the probes with the local flow direction occurred because of the source-flow nature of the external flow. The maximum misalignment was about 3° at the highest probe elevation ($y \sim 2.0$ in., $x = 4.5$ in.). In order to determine the effect of flow angularity on the thin-wire probe data in these experiments, several additional runs were made with probes positioned in the nozzle freestream, at a point corresponding to the $x = 4.5$ in. station on the plate, and oriented with respect to the flow direction at angles up to 7°. No influence of probe orientation was observed.

The voltage applied to the flush probes was swept from -19.5 to $+0.5$ v in the nitrogen plasma and from -17 to $+3$ v in argon, over a period of about 80 μsec. A typical flush-probe ion-current record in argon is shown in Fig. 4. Flush probe data were recorded at both the $x = 4.5$ in. and 9.5 in. plate stations in order to investigate the behavior of the collected ion current with axial distance from the plate leading edge. During the course of the experiments, the absence of probe interference effects was confirmed by comparing the probe characteristics of a selected flush probe when the adjacent spanwise flush probes were either swept or allowed to assume the floating potential. Throughout these experiments, a single constant-voltage (-1 v) thin-wire probe was positioned about $\frac{1}{2}$-in. above and aft of the flush probe stations to monitor the arrival time and uniformity of the test plasma. This ensured proper synchronization of the applied voltage ramp with the plasma interval over the flush probes.

The ranges of the pertinent parameters for the flat-plate experiments in the expanding nozzle flows are summarized as follows: a) electron number density, (cm^{-3}) $10^9 < n_{e_\infty} < 6 \times 10^{11}$; b) Mach number $7 < M_\infty < 20$; c) Reynolds number, $280 < Re/cm < 3600$; d) electron to translational temperature ratio, $3 < T_e/T_i < 10$; e) flush probe radius to Debye length ratio $3 < R/\lambda_D < 4000$; f) flush probe radius to local sheath thickness ratio $0.01 < R/\lambda_s < 20$; g) local sheath thickness to boundary-layer thickness ratio, $0.05 < \lambda_s/\delta < 0.5$; h) applied probe potential, (volts) $-20 < V_p < 3$.

Table 2 Flow parameters behind incident shock wave in nitrogen

p_1, torr	M_i	p_2, mm Hg	ρ_2, g/cm^3	$T_2(=T_e)$, °K	U_2, m/sec	μ_2, poise	Re, cm^{-1}	n_e, cm^{-3}
1	9.2	102	1.08×10^{-5}	4200	2815	10.1×10^{-4}	3020	1.35×10^{10}
1	9.67	111	1.11	4450	2965	10.45	3145	5×10^{10}
1'	9.79	115	1.13	4510	3020	10.55	3225	6.7×10^{10}

The current collection to swept-voltage flush probes under conditions of equal electron and heavy-particle temperatures was investigated in a series of experiments performed in the equilibrium flow behind the incident shock wave in the 6-in.-diam shock tube. The 3 x 3-in. flat plate used by Burke[7] was employed in these studies, with nitrogen used as the test gas. The $\frac{1}{4}$-in.-diam probes were swept from -19 to $+1$ v following passage of the incident shock wave and the shock tube conditions were selected to provide a range of number densities comparable to those obtained in the nozzle experiments. The equilibrium flow parameters in the shock tube experiments are shown in Table 2.

Results and Discussion

The results of the above experiments and analyses are shown in Figs. 6–15. The electron temperature distribution measured in the expanding nitrogen plasma by means of the thin-wire probes is shown in Fig. 6. The electron temperatures are seen to be significantly higher than the heavy-particle translational temperature, which has been included in the figure for comparison, because of energy transfer processes between the electrons and the parent gas. Hurle and Russo[29] have shown that the primary source of electron energy in expanding nitrogen plasmas is that due to vibrational energy exchange with the nitrogen molecule. In order to measure the nitrogen vibrational temperature in the expanding nitrogen plasma, a complementary series of experiments were performed at the conclusion of the present studies. These experiments comprised infrared band-reversal temperature measurements using CO as thermometric additive, and line-reversal measurements using a trace of chromium carbonyl as additive. Preliminary results show $T_{vib} > T_e$ at the two nozzle stations (Fig. 6). Details of these reversal-temperature measurements will be reported later. The freestream electron temperature distribution was not measured in the argon plasma. However, the profile measurements to be discussed also show the electron temperature to be considerably higher than the translational temperature. The electron thermal energy source in the argon plasma was most probably due to the small (0.12%) nitrogen additive in this case.

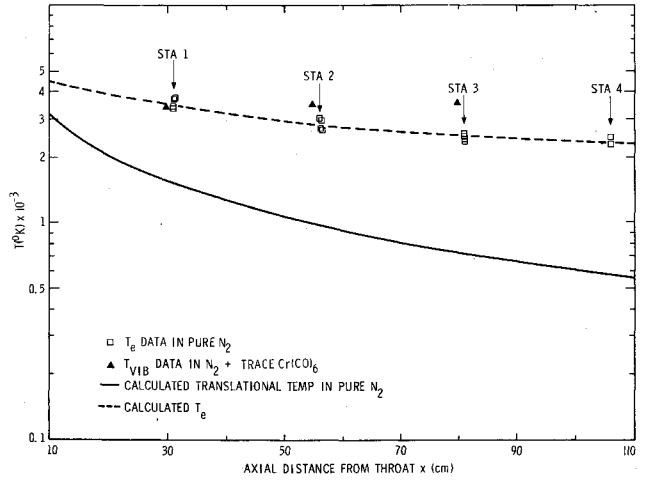

Fig. 6 Measured electron and vibrational temperatures in expanding nitrogen plasma.

Flat Plate n_e, T_e Profiles

The measured n_e-profiles in the flat plate boundary layer are shown in Figs. 7 and 8 for N_2 and Ar, respectively. They exhibit a viscous shock layer type profile at the 4.5 in. station and subsequently relax to Blasius-type flat plate boundary layer profiles at the 9.5 in. station. Computations using Blottner's[24] nonequilibrium program adapted to flat plate flows, using a separate electron energy equation show reasonably good agreement with the n_e-data (solid lines). The T_e-profiles measured over the flat plate in N_2 and Ar are shown in Fig. 9 and illustrate a significant departure from thermal equilibrium with T_e remaining essentially constant in the boundary layer. For nitrogen, $T_e \sim$ 2300–2800°K and for argon, $T_e \sim$ 1000–1500°K.

Flush-Probe Current-Voltage (CV) Characteristics

Although both positive and negative saturation currents were obtained, the CV characteristics emphasized ion-current collection at negative probe potentials. Figure 10 shows several CV characteristics with dimensional probe current plotted against the dimensionless probe potential φ_p. The resulting curves are seen to be nonlinear and illustrate the complex nature of the CV characteristics in that current collection depends on n_e, R_e, probe size and φ_p.

Three distinct but related phenomena are responsible for this behavior. The first is the collisional effect in the sheath, be it thick or thin relative to probe size R, or boundary-layer thickness δ. The second is a probe size effect which is clearly visible in Fig. 10. Compare the slopes of the 0.132- and 1.25-in. probes. The third is a thick sheath effect, that depends primarily on the λ_s/δ ratio. This effect can be observed by the noticeable increase in the slopes of the CV curves as the probe potential increases. In fact, the increase in slope is relatively sudden and was predicted by Stahl and Su in their numerical solution of the Blasius profile (dash-dot curves in Fig. 10; see also Ref. 30: Fig. 4). The φ_p value at which the change in slope occurs depends directly upon the value of $\varkappa$ which is inversely proportional to Re (or directly to δ^2). In addition, the local sheath thickness $\lambda_s \propto \varphi_p^{1/2}$. As δ increases, $\varkappa$ increases and in order to effect a change such that $\lambda_s = 0(\delta)$ (and hence the increase in slope), φ_p must increase.

The nonlinear behavior of the CV characteristics, makes it hard to relate J to φ_p, explicitly. Reference to Fig. 10, however, shows that at low φ_p values, the characteristics are approximately linear on a log-log plot, whence the slopes m (Fig. 11) are independent of φ_p over a certain ($-2 \leq v < -8$) range and functions

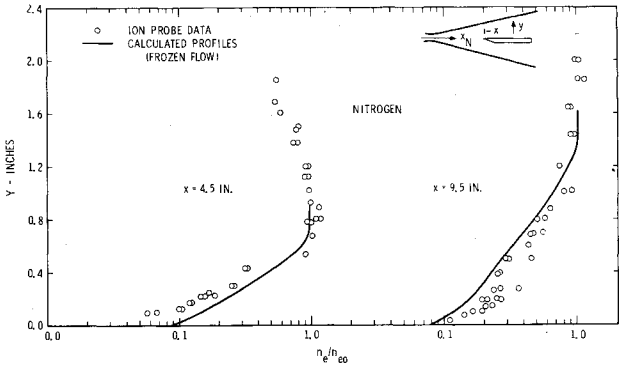

Fig. 7 Calculated and measured N_e-profiles over flat plate in N_2.

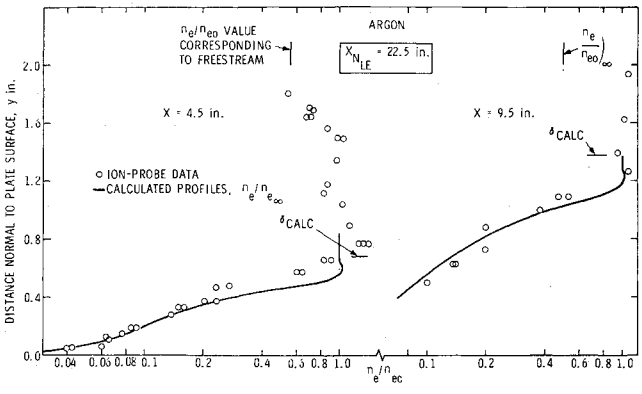

Fig. 8 Calculated and measured N_e-profiles over flat plate in Ar.

only of $\varkappa$, i.e., the effect of sheath thickness is subordinate to the effects of probe size. Under these circumstances, it is seen that the present slope data may be fitted with the same type of empirical curve (e.g., $m = [1 + 4 \ln (1 + 0.5\,\varkappa^{1/2})]^{-1}$ found to describe the potential dependence in the continuum spherical probe experiments of French et al.[31] However, the increase in slope at constant $\varkappa$ for the higher φ_p data in these figures represents the predominant influence of the bias potential on the sheath thickness (of Fig. 10). At these higher values of φ_p the slopes are no longer a function of $\varkappa$ alone and preclude a slope correlation similar to that applicable for low φ_p data.

In an approximate manner, therefore, as one moves from right to left (decreasing $\varkappa$) the Re effects gradually yield to probe size (R/λ_D) effects.

Probe Size and Geometry Effects

Figures 12 and 13 show the probe area effect on the ion current density J. The current density increases as the probe size decreases in agreement with the observations of Tseng and Talbot,[32] and Lederman and Avidor.[13] The former studies were performed under collisionless sheath conditions and the results interpreted in terms of a free-fall sheath thickness $\lambda_s \propto \varphi_p^{3/4}$. For collisional thick sheaths, the present calculations indicate $\lambda_s \propto \varphi_p^{1/2}$. The calculated current density (Fig. 13, solid curve) was obtained using the full, two-dimensional expression for J, (see Ref. 33).

$$J = en_{eo}D_i\left[\left(\frac{\nabla N_e}{\beta} - \nabla N_i\right) + \left(\frac{N_i}{\varepsilon} + \frac{N_e}{\beta}\right)\nabla\psi\right] \qquad (1)$$

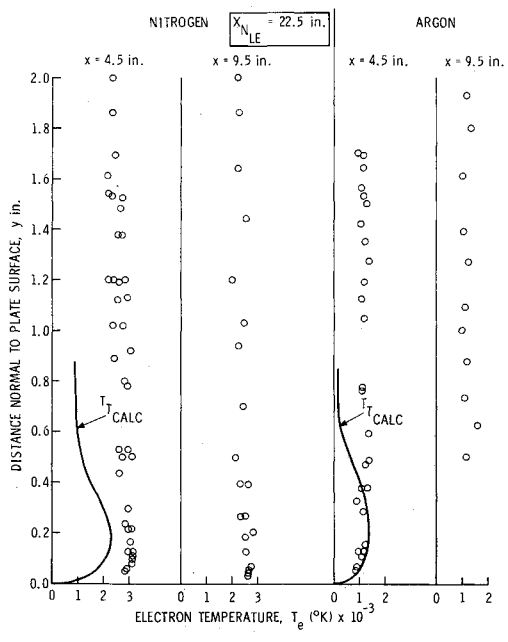

Fig. 9 Calculated and measured T_e-profiles over flat plate in N_2 and Ar.

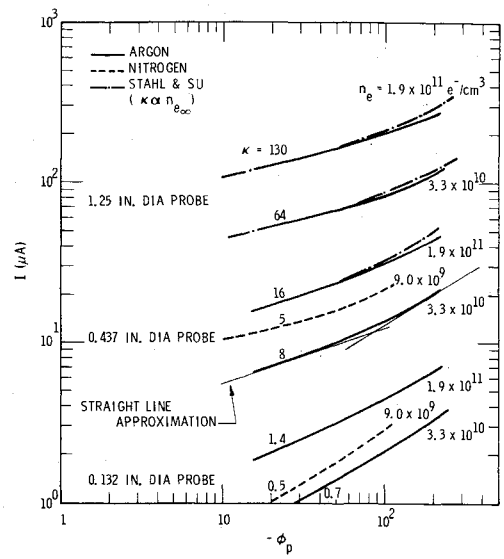

Fig. 10 Current-voltage characteristics for several probes in N_2 and Ar; comparison with theory.

Numerical calculations (see Ref. 33, Fig. 6) show clearly the "fringing" effect that is responsible for the increase in J as the probe area decreases, with φ_p held constant. Figures 12 and 13 further show that the effect of field fringing is noticeably smaller for the collision-dominated sheaths than for the collisionless sheath situation.

Within the limited amount of measurements taken and the data scatter, the ion current density showed no observable dependence on the probe geometry (see also Ref. 13).

Flush-Probe Data Correlation

From collisional thin sheath analyses over flat plates, one obtains the following nondimensional group

$$J' = J_i Sc_i (Re_{x,o})^{1/2}/n_e e U_o \qquad (2)$$

Figures 14 and 15 show the flush probe data correlated in terms of a modified form of this parameter $(Sc_i Re_{xo})^{1/2}$ plotted against R/λ_D (λ_D-based on boundary-layer edge conditions). Data from Refs. 7, 8, and 13 are included in Fig. 14 for the purpose of comparison. The over-all correlation appears satisfactory, and the data in Figs. 14 and 15 exhibit the following trends: 1) for $R/\lambda_D > 10^3$, the J' parameter is approximately constant but increases steadily as R/λ_D decreases and probe size effects become significant, 2) fully equilibrium flows with $T_e = T_i$ (shock tube data) yield higher current densities than frozen flows (shock tunnel data), because of steeper concentration gradients at the sheath edge as shown from analysis,[5] 3) as evidenced in Fig. 14, the low-density data ($n_e < 5 \times 10^9$ cm^{-3}) tend to break away from the J' correlation and show better agreement with the

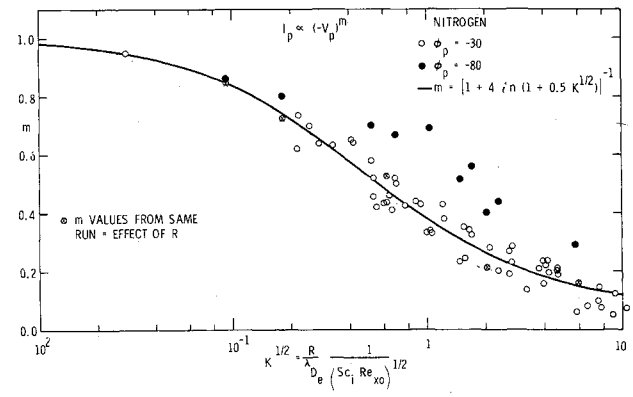

Fig. 11 Current-voltage slopes in N_2, CO, and Ar for applied potential range $8 \leq -\varphi_p < 30$.

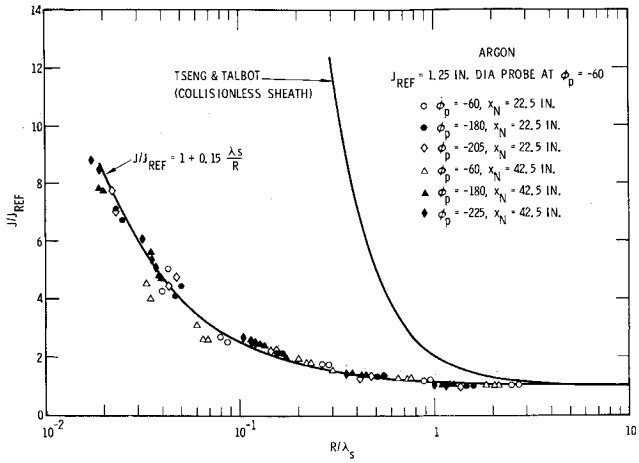

Fig. 12 Area effect on collected current density in argon.

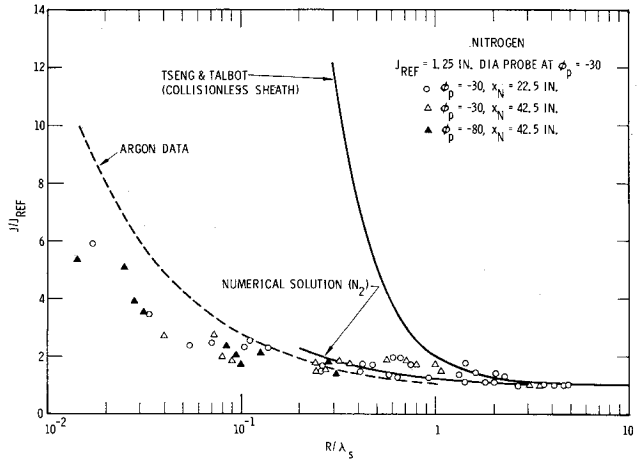

Fig. 13 Area effect on collected current density in nitrogen.

$\frac{2}{3}$-power of the product Sc_iRe_{xo}, appropriate for the thicker sheath situation. This type of dependence was observed by Scharfman and Hammitt[15] on conical probes, 4) finally, as shown by Stahl and Su,[5] one can extract the following type of dependence for the current density J_i on n_e: for $\varphi_p = -30$, $J_i \propto n_{eo}^{0.85-0.90}$ and for $\varphi_p \simeq -100$, $J_i \propto n_{eo}^{0.80-0.85}$. Although it was shown above that $J_i \propto \varphi_p^m$, where $0.1 < m < 1.0$, most of the data can be correlated reasonably well by setting $m = 0.5$ (Fig. 15). It is interesting to note that dividing J' by $\varphi_p^{1/2}$ is equivalent to using the local sheath thickness λ_s instead of the freestream Debye length λ_D for the abscissa.

Summary and Application

Most of the experimental data obtained to date in the flush-mounted probes have been analysed and exhibited in the present paper. From the above data and the available numerical solutions,[33] it is clear that no simple dependence of the flush-probe ion current on the pertinent individual parameters will suffice for the parameter ranges investigated. However, from an over-all correlation, ion current densities may be described to a reasonable approximation by

$$J_i(Sc_iRe_{xo})^{1/2}/n_{eo}eU_o = \text{const}\,(\lambda_D/R)^q(-\varphi_p)^m(1 + T_e/T_i)^{1.2} \qquad (3)$$

where $0.30 \leq q \leq 0.50$

$$m = \{1 + 4\ln[1 + 0.5(\varkappa)^{1/2}]\}^{-1} \simeq 0.5$$

It should be noted that charged particle profiles in the present set of experiments correspond to profiles on relatively blunt re-entry vehicles where ionization occurs primarily in the shock layer. There are, however, a number of re-entry cases where the inviscid outer flow is nearly un-ionized and the charged particle density profiles are dominated by generation within the boundary layer. For such cases, the freestream Debye length λ_D used in the preceding correlations should be replaced either by a Debye length relative to peak ionization or, by the local sheath thickness λ_s as discussed above. [Note from Eq. (3) that $J_i \propto \lambda_D^q\varphi_p^{0.5}$ and $\lambda_s \propto \lambda_D^{2/3}\varphi^{0.5}$.] Another possibility is to use the ion mass fraction profile at the sheath edge. For the thick sheaths encountered in the present set of experiments, however, λ_s is a complicated function of the applied bias and there is no unambiguous way of relating the current density to ion mass fraction at the sheath edge, which now would be an appreciable part of the boundary-layer thickness [see Eq. (2)].

References

[1] Chen, F. F., *Plasma Diagnostic Techniques*, edited by Huddlestone and Leonard, Academic Press, New York, 1965, p. 113.

[2] Lam, S. H., "A General Theory for the Flow of Weakly Ionized Gases," *AIAA Journal*, Vol. 2, No. 2, Feb. 1964, pp. 256–262.

[3] Chung, P. M., "Weakly Ionized Nonequilibrium Viscous Shock-Layer and Electrostatic Probe Characteristics," *AIAA Journal*, Vol. 3, No. 5, May 1965, pp. 817–825.

[4] Denison, M. R., "Analysis of Flush Electrostatic Probes for Reentry Measurements," Rept. 06488-6065-R000, Sept. 1967, TRW Systems, Redondo Beach, Calif.

[5] Burke, A. F., "Theoretical Studies of Continuum, Weakly Ionized Gas Flows including Compressibility and Electron Energy Effects," Rept. AN-2101-Y-1, May 1967, Cornell Aeronautical Lab., Buffalo, N. Y.

[6] Hoppmann, R. F., "Cold Electrode Characteristics in Shock-

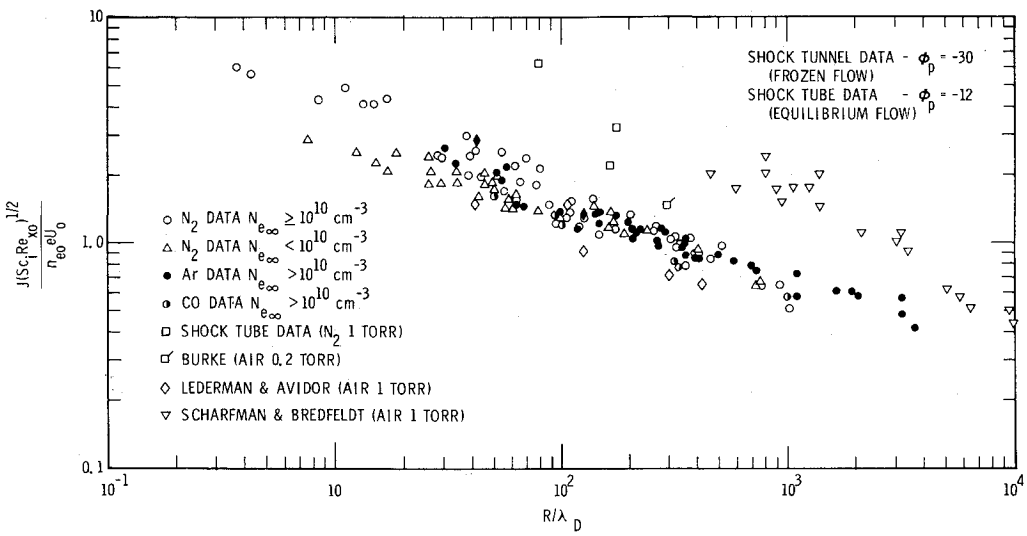

Fig. 14 Nondimensional current density vs dimensionless probe size; a composite plot.

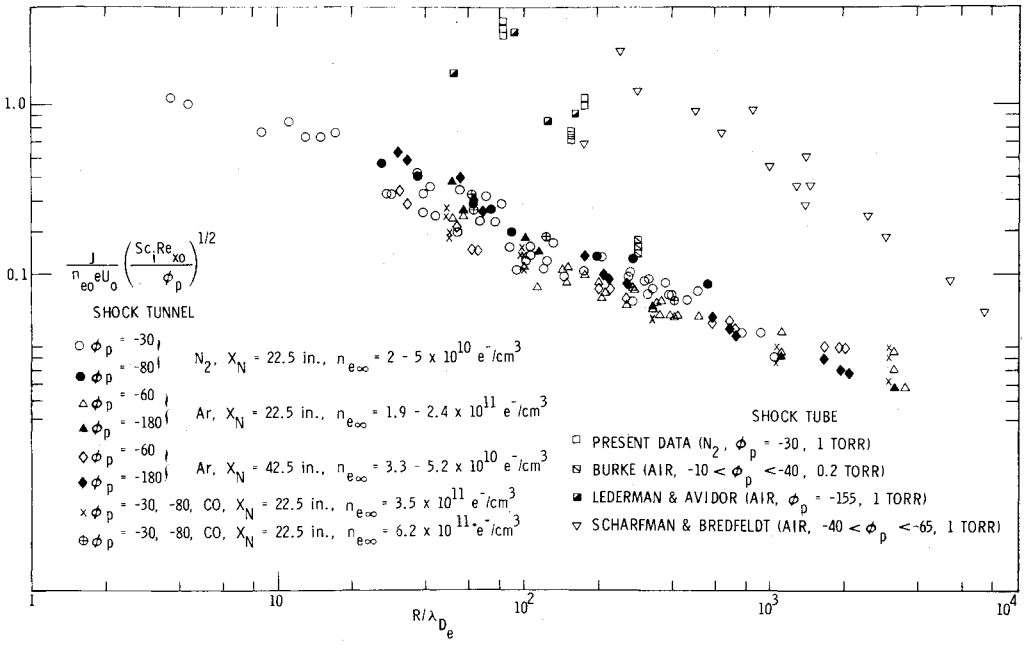

Fig. 15 Nondimensional current density vs dimensionless probe size; a composite plot with φ_p included.

Ionized Plasmas," *The Physics of Fluids*, Vol. 11, No. 5, May 1968, pp. 1092–1100.

[7] Burke, A. F., "Electrical Currents to a Flat Plate in a Supersonic Ionized Flow," AIAA Paper 68-166, New York, 1968.

[8] Scharfman, W. E. and Bredfeldt, H. R., "Experimental Investigation of Flush-Mounted Electrostatic Probes," *AIAA Journal*, Vol. 8, No. 4, April 1970, pp. 662–665.

[9] Sonin, A. A., "Theory of Ion Collection by a Supersonic Atmospheric Sounding Rocket," *Journal of Geophysical Research*, Vol. 72, No. 17, Sept. 1967, pp. 4547–4557.

[10] deBoer, P. C. T. and Johnson, R. A., "Theory of Flat-Plate Ion-Density Probe," *The Physics of Fluids*, Vol. 11, No. 4, April 1968, pp. 909–911.

[11] Dukowicz, J. K., "Theory of Convection-Conduction Dominated Electrostatic Probes: Numerical Solution of the Two-Dimensional Flat Plate Problem," Rept. RA-2641-Y-1, Jan. 1969, Cornell Aeronautical Lab., Buffalo, N. Y.

[12] Hammitt, A. G., "Negatively Charged Electrostatic Probes in High Density Plasma," Rept. 06488-6433-R0-00, June 26, 1970, TRW Systems, Redondo Beach, Calif.

[13] Lederman, S. and Avidor, J., "The Application of Flush Mounted Electrostatic Probes to Flow Diagnostics," *Israel Journal of Technology* Vol. 9, Nos. 1–2, 1971, pp. 19–28.

[14] Dukowicz, J. K., "Conical Electrostatic Probes in a Continuum Flowing Plasma," Rept. AN-2755-Y-1, Jan. 1970, Cornell Aeronautical Lab., Buffalo, N. Y.

[15] Scharfman, W. E. and Hammitt, A. G., "Experimental Determination of the Characteristics of Negatively Charged Conical Electrostatic Probes in a Supersonic Flow," *AIAA Journal*, Vol. 10, No. 4, April 1972, pp. 434–439.

[16] Dunn, M. G. and Lordi, J. A., "Measurement of $N_2^+ + e^-$ Dissociative Recombination in Expanding Nitrogen Flows," Rept. AL-2187-A-13, April 1969, Cornell Aeronautical Lab., Buffalo, N. Y.; also *AIAA Journal*, Vol. 8, No. 2, Feb. 1970, pp. 339–345.

[17] Dunn, M. G. and Lordi, J. A., "Development of Free-Molecular Langmuir Probes for Measurement of Electron Temperature and Number Density in Shock-Tunnel Flows," Rept. AN-2101-Y-2, May 1968, Cornell Aeronautical Lab., Buffalo, N. Y.; also *AIAA Journal*, Vol. 7, No. 8, August 1969, pp. 1458–1465.

[18] Lordi, J. A., Mates, R. E. and Moselle, J. R., "Computer Program for the Numerical Solution of Nonequilibrium Expansions of Reacting Gas Mixtures," Rept. AD-1689-A-6, June 1965, Cornell Aeronautical Lab., Buffalo, N. Y.

[19] Burke, A. F. and Wallace, J. E., "Aerothermodynamic Consequences of Nozzle Nonequilibrium," Rept. AM-1906-Y-1, Jan. 1966, Cornell Aeronautical Lab., Buffalo, N. Y.

[20] Sonin, A. A., "The Behavior of Free-Molecule Cylindrical Langmuir Probes in Supersonic Flows, and the Application to the Study of the Blunt-Body Stagnation Layer," Rept. 109, Aug. 1965, Inst. for Aerospace Studies, Univ. of Toronto, Toronto, Canada.

[21] Dunn, M. G., "Measurement of $C^+ + e^- + e^-$ Three-Body Recombination in $CO^+ + e^-$ Dissociative Recombination in Expanding Carbon Monoxide Flows," *AIAA Journal*, Vol. 9, No. 11, Nov. 1971, pp. 2184–2191.

[22] Boyer, D. W., "Experimental Studies of Flush-Mounted Electrostatic Probes in Collision-Dominated Hypersonic Ionized Flows," Rept. SC-CR-72-3145, June 1972, Sandia Labs., Albuquerque, N. Mex.

[23] Burke, A. F. and Bird, K. D., "The Use of Conical and Contoured Expansion Nozzles in Hypervelocity Facilities," Rept. 112, (revised version) July 1962, Cornell Aeronautical Lab., Buffalo, New York.

[24] Blottner, F. G., "Finite Difference Methods of Solution of the Boundary-Layer Equations," *AIAA Journal*, Vol. 8, No. 2, Feb. 1970, pp. 193–205.

[25] Dunn, M. G. and Lordi, J. A., "Thin-Wire Langmuir-Probe Measurements in the Transition and Free-Molecular Flow Regimes," *AIAA Journal*, Vol. 8, No. 6, June 1970, pp. 1077–1081.

[26] Laframboise, J. G., "Theory of Spherical and Cylindrical Langmuir Probes in a Collisionless, Maxwellian Plasma at Rest," Rept. 100, March 1966, Inst. for Aerospace Studies, Univ. of Toronto, Toronto, Canada.

[27] Hester, S. D. and Sonin, A. A., "Ion Temperature Sensitive End Effect in Cylindrical Langmuir Probe Response at Ionospheric Satellite Conditions," *The Physics of Fluids*, Vol. 13, No. 5, May 1970, pp. 1265–1274.

[28] Talbot, L. and Chou, Y. S., "Langmuir Probe Response in the Transition Regime," Sixth Rarefied Gasdynamics Symposium, Boston, Mass., June 1968.

[29] Hurle, I. R. and Russo, A. L., "Spectrum-Line Reversal Measurements of Free-Electron and Coupled N_2 Vibrational Temperatures in Expansion Flows," *The Journal of Chemical Physics*, Vol. 43, No. 12, Dec. 1965, pp. 4434–4443.

[30] Stahl, N. and Su, C. H., "Theory of Continuum Flush Probes," *The Physics of Fluids*, Vol. 14, No. 7, July 1971, pp. 1366–1376.

[31] French, I. P. et al., "Calibration and Use of Electrostatic Probes for Hypersonic Wake Studies," *AIAA Journal*, Vol. 8, No. 12, Dec. 1970, pp. 2207–2214.

[32] Tseng, R. C. and Talbot, L., "Flat Plate Boundary-Layer Studies in a Partially Ionized Gas," *AIAA Journal*, Vol. 9, No. 7, July 1971, pp. 1365–1372.

[33] Russo, A. J. and Touryan, K. J., "Experimental and Numerical Studies of Flush Electrostatic Probes in Hypersonic Ionized Flows: II. Theory," *AIAA Journal*, Vol. 10, No. 12, Dec. 1972, pp. 1675–1678.